

CHAPTER

15

COMPUTED TOMOGRAPHY

OBJECTIVES	252	COLLIMATION	258
INTRODUCTION	252	X-RAY DETECTORS	258
HISTORY	252	VIEWING SYSTEMS	258
PRINCIPLE OF COMPUTED TOMOGRAPHIC IMAGING	253	PATIENT DOSE	259
RECONSTRUCTION ALGORITHMS	254	QUALITY CONTROL	260
SCAN MOTIONS	255	SUMMARY	262
First- to Fourth-Generation CT Scanners	255	PROBLEMS	262
Spiral CT Scanning	255	REFERENCES	262
Ultrafast CT Scanners	256		
X-RAY SOURCES	258		

OBJECTIVES

After completing this chapter, the reader should be able to:

- Explain the principles of x-ray transmission computed tomography.
- Compare the properties of x-ray projection images with x-ray CT images.
- Provide a brief history of the evolution of x-ray CT imaging.
- Describe different approaches to the reconstruction of CT images from projection measurements.
- Depict the configuration of spiral and “ultrafast” CT scanners.
- Outline the features of x-ray sources, detectors, collimators, and display systems used in x-ray CT.
- Characterize the relationship between CT numbers, linear attenuation coefficients, and physical densities associated with CT scanning.
- Identify various characteristics important in quality control of CT units.

INTRODUCTION

In conventional radiography, subtle differences of less than about 5 percent in subject contrast (i.e., x-ray attenuation in the body) are not visible in the image. This limitation exists for the following reasons:

1. The projection of three-dimensional anatomic information onto a two-dimensional image receptor obscures subtle differences in x-ray transmission through structures aligned parallel to the x-ray beam. Although conventional tomography resolves this problem to some degree, structures above and below the tomographic section may remain visible as “ghosts” in the image if they differ significantly in their x-ray attenuating properties from structures in the section.
2. Conventional image receptors (i.e., film, intensifying and fluoroscopic screens) are not able to resolve small differences (e.g., 2%) in the intensity of incident radiation.
3. Large-area x-ray beams used in conventional radiography produce considerable scattered radiation that interferes with the display of subtle differences in subject contrast.

To a significant degree, each of these difficulties is eliminated in computed tomography (CT). Hence, differences of a few tenths of a percent in subject contrast are revealed in the CT image. Although the spatial resolution of a millimeter or so provided by CT is notably poorer than that provided by conventional radiography, the superior visualization of subject contrast, together with the display of anatomy across planes (e.g., cross-sectional) that are not accessible by conventional imaging techniques, make CT exceptionally useful for visualizing anatomy in many regions of the body.

HISTORY

The image reconstruction techniques used in CT were developed for use in radio astronomy,¹ electron microscopy,² and optics including holographic interferometry.^{3–5} In 1961, Oldendorf explored the principle of CT with an apparatus using an ¹³¹I source.⁶ Shortly thereafter, Kuhl and colleagues developed emission and ²⁴¹Am transmission CT imaging systems and described the application of these systems to brain imaging.^{7,8} In spite of these early efforts, CT remained unexploited for clinical imaging until the announcement by EMI Ltd. in 1972 of the first commercially available x-ray transmission CT unit designed exclusively for studies of the head.⁹ The prototype for this unit had been studied since 1970 at Atkinson–Morley

The term “tomography” is derived from the Greek word *tomos*, meaning “section.”

Computed tomography was not the first x-ray method to produce cross-sectional images. In the late 1940s and 1950s, Takahashi in Japan published several papers describing the analog technique of transverse axial tomography. Takahashi’s method was commercialized by Toshiba Inc. in the 1960s. The Toshiba product was usurped by computed tomography in the early 1970s.

William Oldendorf was a neuroscientist interested in improving the differentiation of brain tissue. In particular, he was searching for a better imaging method than pneumoencephalography for studying the brain. Many scientists believe he should have shared the 1970 Nobel Prize in Medicine.

The 1970 Nobel Prize in Medicine was shared by two pioneers of computed tomography, Godfrey Hounsfield, an engineer with EMI Ltd., and Allen Cormack, a South African medical physicist.

Hounsfield was a radar instructor during World War II. Before developing the first x-ray CT scanner, he designed the first transistorized digital computer while working as an engineer at EMI Ltd.

Hospital in England, and the first commercial unit was installed in the United States in 1973. The same year, Ledley and colleagues announced the development of a whole-body CT scanner.¹⁰ In 1974, Ohio Nuclear Inc. also developed a whole-body CT scanner, and clinical models of both units were installed in 1975. By 1977, 16 or so commercial companies were marketing more than 30 models of transmission CT scanners. Today, approximately 5000 CT units are installed in U.S. hospitals, at a cost of up to a million dollars or slightly more per unit.

■ PRINCIPLE OF COMPUTED TOMOGRAPHIC IMAGING

In early CT imaging devices (“scanners”) a narrow x-ray beam is scanned across a patient in synchrony with a radiation detector on the opposite side of the patient. If the beam is monoenergetic or nearly so, the transmission of x rays through the patient is

$$I = I_0 e^{-\mu x}$$

In this equation the patient is assumed to be a homogeneous medium. If the x-ray beam is intercepted by two regions with attenuation coefficients μ_1 and μ_2 and thicknesses x_1 and x_2 , the x-ray transmission is

$$I = I_0 e^{-(\mu_1 x_1 + \mu_2 x_2)}$$

If many (n) regions with different linear attenuation coefficients occur along the path of x-rays, the transmission is

$$I = I_0 e^{-\sum_{i=1}^n \mu_i x_i}$$

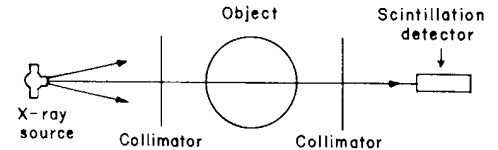
where $-\sum_{i=1}^n \mu_i x_i = (\mu_1 x_1 + \mu_2 x_2 + \dots + \mu_n x_n)$, and the fractional transmission I/I_0 is

$$e^{-\sum_{i=1}^n \mu_i x_i}$$

With a single transmission measurement, the separate attenuation coefficients cannot be determined because there are too many unknown values of μ_i in the equation. However, with multiple transmission measurements in the same plane but at different orientations of the x-ray source and detector, the coefficients can be separated so that a cross-sectional display of attenuation coefficients is obtained across the plane of transmission measurements. By assigning gray levels to different ranges of attenuation coefficients, a gray-scale image can be produced that represents various structures in the patient with different x-ray attenuation characteristics. This gray-scale display of attenuation coefficients constitutes a CT image.

In early (first-generation) CT scanners, multiple x-ray transmission measurements are obtained by scanning a pencil-like beam of x rays and an NaI detector in a straight line on opposite sides of the patient (Figure 15-1A). During this translational scan of perhaps 40 cm in length, multiple (e.g., 160) measurements of x-ray transmission are obtained. Next, the angular orientation of the scanning device is incremented 1 degree, and a second translational scan of 160 transmission measurements is performed. This process of translational scanning separated by 1-degree increments is repeated through an arc of 180 degrees. In this manner, $160 \times 180 = 28,800$ x-ray transmission measurements are accumulated. These measurements are transmitted to a computer equipped with a mathematical package for reconstructing an image of attenuation coefficients across the anatomic plane defined by the scanning x-ray beam.

Cormack was interested in the generation of cross-sectional displays of attenuation coefficients for use in treatment planning for radiation therapy. He published his results in the *Journal of Applied Physics*. He received only one reprint request. It was from members of the Swiss Avalanche Research Center, who were interested in possible use of his method to predict snow depths.



MARGIN FIGURE 15-1

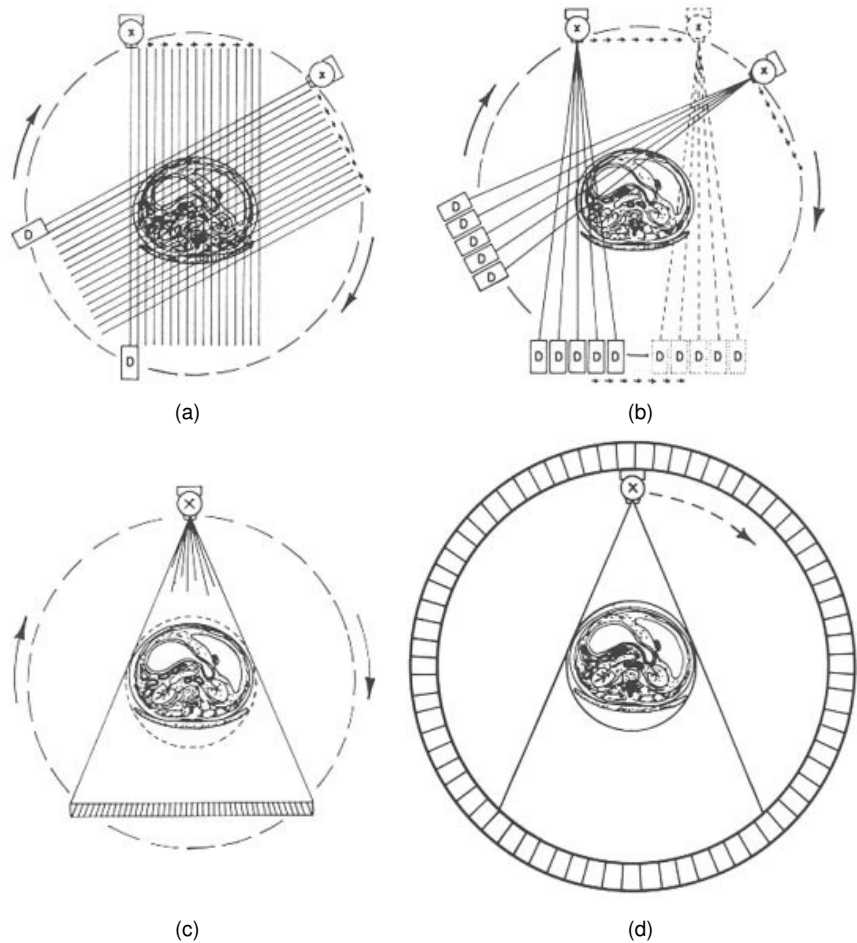
In a first-generation computed tomographic scanner, x-ray transmission measurements are accumulated while an x-ray source and detector are translated and rotated in synchrony on opposite sides of the patient.

Hounsfield termed his technique “computerized transverse axial tomography.” This expression was later abbreviated to “computerized axial tomography,” and was referred to as “CAT scanning.” After sufficient ridicule had been directed toward this acronym, the expression *computed tomography* (CT scanning) was adopted by major journals in medical imaging.

X-ray CT images are often described as “density distributions” because they provide a gray-scale display of linear attenuation coefficients that are closely related to the physical density of tissues.

The scanning technique employed by first generation CT scanners is referred to as “rectilinear pencil-beam scanning.”

The first five clinical CT units marketed by EMI Ltd. were installed by early 1973 in London, Manchester, Glasgow, Rochester (MN), and Boston.

**FIGURE 15-1**

Scan motions in computed tomography. **A:** first-generation scanner using a pencil x-ray beam and a combination of translational and rotational motion. **B:** Second-generation scanner with a fan x-ray beam, multiple detectors, and a combination of translational and rotational motion. **C:** Third-generation scanner using a fan x-ray beam and smooth rotational motion of x-ray tube and detector array. **D:** Fourth-generation scanner with rotational motion of the x-ray tube within a stationary circular array of 600 or more detectors.

Backprojection is also known as the *summation method* or the *linear supposition method*.

Simple backprojection does not produce sharp and clear images, and it is not used in commercial CT scanners.

The integral equations approach to image reconstruction was first described in 1917 by the Austrian mathematician Radon. He developed his equations for studies of gravitational fields.¹²

As used in a mathematical sense, the word *filter* connotes a mathematical operation on a set of data. The convolution filter (also called a *kernel*) discussed here is applied to the data before they are backprojected to form an image.

RECONSTRUCTION ALGORITHMS

The foundation of the mathematical package for image reconstruction is the reconstruction algorithm, which may be one of four types.¹¹

1. *Simple backprojection.* In this method, each x-ray transmission path through the body is divided into equally spaced elements, and each element is assumed to contribute equally to the total attenuation along the x-ray path. By summing the attenuation for each element over all x-ray paths that intersect the element at different angular orientations, a final summed attenuation coefficient is determined for each element. When this coefficient is combined with the summed coefficients for all other elements in the anatomic section scanned by the x-ray beam, a composite image of attenuation coefficients is obtained. Although the simple backprojection approach to reconstruction algorithms is straightforward, it produces blurred images of sharp features in the object.
2. *Filtered backprojection.* This reconstruction algorithm, often referred to as the *convolution* method, uses a one-dimensional integral equation for the

reconstruction of a two-dimensional image. In the convolution method of using integral equations, a deblurring function is combined (convolved) with the x-ray transmission data to remove most of the blurring before the data are backprojected. The most common deblurring function is a filter that removes the frequency components of the x-ray transmission data that are responsible for most of the blurring in the composite image. One of the advantages of the convolution method of image reconstruction is that the image can be constructed while x-ray transmission data are being collected. The convolution method is the most popular reconstruction algorithm used today in CT.

3. *Fourier transform.* In this approach, the x-ray attenuation pattern at each angular orientation is separated into frequency components of various amplitudes, similar to the way a musical note can be divided into relative contributions of different frequencies. From these frequency components, the entire image is assembled in “frequency space” into a spatially correct image and then reconstructed by an inverse Fourier transform process.
4. *Series expansion.* In this technique, variations of which are known as ART (algebraic reconstruction technique), ILST (iterative least-squares technique), and SIRT (simultaneous iterative reconstruction technique), x-ray attenuation data at one angular orientation are divided into equally spaced elements along each of several rays. These data are compared with similar data at a different angular orientations, and differences in x-ray attenuation at the two orientations are added equally to the appropriate elements. This process is repeated for all angular orientations, with a decreasing fraction of the attenuation differences added each time to ensure convergence of the reconstruction data. In this method, all x-ray attenuation data must be available before reconstruction can begin.

A high-frequency convolution filter reduces noise and makes the image appear “smoother.” A low-frequency filter enhances edges and makes the image appear “sharper.” A low-frequency filter may be referred to as a “high-pass” filter because it suppresses low frequencies and allows high frequencies to pass.

Filtered backprojection removes the star-like blurring seen in simple backprojection. It is the principal reconstruction algorithm used in CT scanners.

The Fourier approach to image reconstruction is used commonly in magnetic resonance imaging, but seldom in CT scanning.

In 1958, the Ukrainian physicist Korenblyum¹³ from the Kiev Polytechnic Institute reworked Radon's integral equations for application to fan-beam geometry. He verified his approach with images of a rotating body captured on film.

Series expansion (iterative reconstruction) techniques are not used in commercial CT scanners because the iteration cannot be started until all of the projection data have been acquired, causing a delay in reconstruction of the image.

The first CT scan of a patient was acquired at London's Atkinson-Morley Hospital in 1972.

In the mid-1970s more than 20 companies were developing x-ray CT scanners for the clinical market. Today, CT scanners are manufactured only by large international manufacturers of x-ray imaging equipment.

Because of their extended data acquisition and image reconstruction times, first- and second-generation CT scanners were limited principally to studies of the head and extremities where methods to immobilize anatomy could be employed.

Development of a purely rotational CT scanner required a more complex reconstruction algorithm that accommodated a purely rotational geometry. This algorithm was developed in the mid-1970s by scientists at General Electric Medical Systems.

■ SCAN MOTIONS

First- to Fourth-Generation CT Scanners

Early (*first-generation*) CT scanners used a pencil-like beam of x-rays and a combination of translational and rotational motion to accumulate the many transmission measurements required for image reconstruction (Figure 15-1A). Although this approach yields satisfactory images of stationary objects, considerable time (4 to 5 minutes) is required for data accumulation, and the images are subject to motion blurring. Soon after the introduction of pencil-like beam scanners, fan-shaped x-ray beams were introduced so that multiple measures of x-ray transmission could be made simultaneously (Figure 15-1B). Fan beam geometries with increments of a few degrees for the different angular orientations (e.g., a 30-degree fan beam and 10-degree angular increments) reduced the scan time to 20 to 60 seconds. Fan beam geometries also improved image quality by reducing the effects of motion. CT scanners with x-ray fan beam geometries and multiple radiation detectors constitute the *second generation* of CT scanners.

The third and fourth generations of CT scanners eliminate the translational motion of previous scanners and rely exclusively upon rotational motion of the x-ray tube and detector array (third generation Figure 15-1, C) or upon rotational motion of the x-ray tube within a stationary circular array of 700 or more detectors (fourth-generation scanner, Figure 15-1D). With these scanners, data accumulation times as short as 1 second are achievable.

Spiral CT Scanning

Several approaches to even faster CT scans have been pursued. Until recently, multiple scan sequences to produce contiguous image “slices” required that the x-ray tube stop its rotation and reverse its direction because the maximum extension of the

Spiral CT scanning is also known as *helical CT scanning*.

Spiral CT scanners today employ multiple detector rings to scan several slices through the body during each gantry rotation. These scanners are referred to as multislice CT scanners.

The principal advantage of spiral CT is its ability to image a larger volume of tissue in a relatively short time. With spiral CT, for example, the entire torso can be imaged in a single breathold.

A pitch of one yields a contiguous spiral. A pitch of two yields an extended spiral. A pitch of $1/2$ yields an overlapping spiral.

Multislice CT scanners have many advantages, but also some disadvantages. Hundreds of CT images can be accumulated in a single study, resulting in high patient doses and massive amounts of digital imaging data.

TABLE 15-1 Advantages of Spiral Compared with Conventional Computed Tomography

<ul style="list-style-type: none"> • Faster image acquisition • Quicker response to contrast media • Fewer motion artifacts • Improved two-axis resolution • Physiological imaging • Improved coronal, sagittal, and 3D imaging • Less partial volume artifact • No misregistration

Research on the dynamic spatial reconstructor has been discontinued.

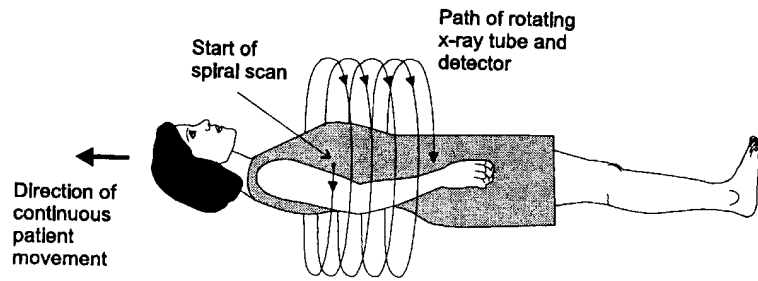


FIGURE 15-2 Spiral CT scanning. (From Rowlands, J.¹⁴ Used with permission.)

high-voltage cables had been reached. Thus, a successive slice-by-slice accumulation technique was used to produce multislice images. In this technique, the total image acquisition time is significantly longer than the beam-on time because the table increments (moves) to the next slice location and the patient breathes between slices.

Spiral CT scanning was introduced in 1989 and is used almost universally today for third- and fourth-generation CT scanning. In this approach, image acquisition time is decreased significantly by connecting the tube voltage cables through a “slip ring” or sliding contact mounted on the rotating gantry of the unit. With slip ring technology, the x-ray tube rotates while the patient table moves without stopping. Hence, the patient is moved continuously through the gantry during the study, and the x-ray beam maps out a helical or spiral path in the patient, as depicted in Figure 15-2. Potential advantages of the spiral CT technique include a reduction of patient motion and a general increase in patient throughput.¹⁵ A greater volume of the patient may be scanned during the passage of contrast media, permitting reduction in the volume of contrast needed. Also, the continuity of data along the axis of the patient (i.e., absence of gaps between scans) improves the quality of three-dimensional reconstruction.¹⁶

In single-slice CT scanning, *pitch* is defined as the *patient couch movement per rotation divided by the slice thickness*. In multislice CT, this definition is altered slightly to *patient couch movement per rotation divided by the beam width*. Low pitch (i.e., small increments of couch movement) yields improved spatial resolution along the long axis (Z axis) of the patient, but also results in higher patient doses and longer imaging times. For pitches greater than unity, the dose to the patient is less, but data must be interpolated so that resolution along the Z axis is preserved. Advantages of spiral over sectional computed tomography are listed in Table 15-1.

Ultrafast CT Scanners

Other approaches to fast CT scanning have involved radically different approaches to equipment design. In the late 1970s the first approach to subsecond CT scans was proposed by a group at the Mayo Clinic.¹⁷ This approach, known as the dynamic spatial reconstructor (DSR), incorporated 28 gantry-mounted x-ray tubes over a 180-degree arc and used an equal number of image intensifier assemblies mounted on the opposite semicircle of the gantry. The entire assembly rotated about the patient at a rate of 15 rpm to provide 28 views every 1/60 second. Working models of the system were built for research,¹⁸ but the technical complexity and cost prevented the DSR from being marketed commercially. A diagram of the DSR is shown in Figure 15-3.

Another approach to fast CT scanning eliminates mechanical motion entirely by converting the gantry of the unit into a giant x-ray tube in which the focal spot moves electronically about the patient.²⁰ This device, known as ultrafast CT (UFCT), cardiovascular CT (CVCT), or “cine CT,” incorporates a semicircular tungsten x-ray target into the gantry.^{21,22} A scanning electron beam with an energy of 130 keV is swept around the semicircular target so that the focal spot moves around the patient. A stationary semicircular bank of detectors records the x-ray transmission in a fashion

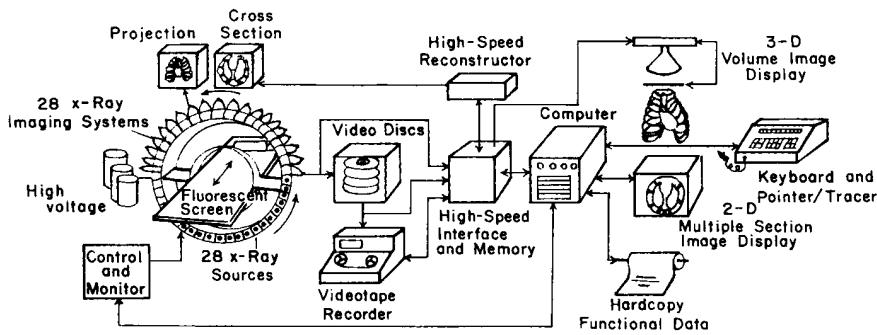
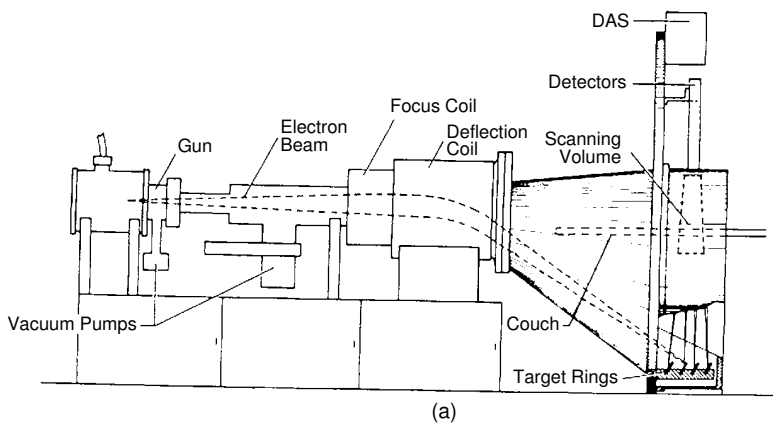


FIGURE 15-3 The dynamic spatial reconstructor. (From Robb, R., Lent, A., and Chu, A.¹⁹ Used with permission.)

similar to that of a fourth-generation scanner. Because of the speed with which the electron beam may be steered magnetically, a scan may be accomplished in as little as 50 ms and repeated after a delay of 9 ms to yield up to 17 images per second.²³ By using four target rings and two detector banks, eight slices of the patient may be imaged without moving the patient. A diagram of a scanning electron beam CT scanner is shown in Figure 15-4.

The UFCT is often referred to as electron-beam computed tomography [EBCT]. It was initially referred to as a cardiovascular CT scanner.



The UFCT unit was developed in the late 1970s by D. Boyd and colleagues at the University of California—San Francisco.

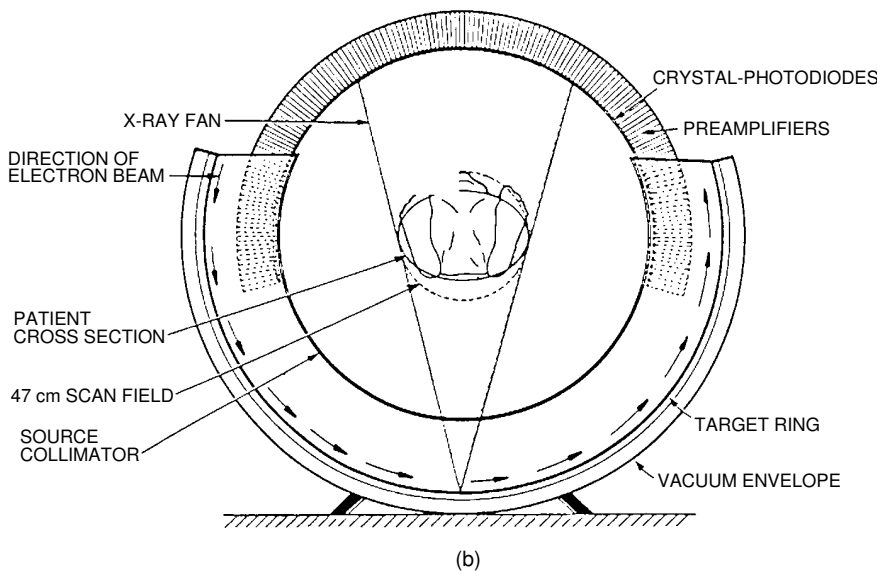


FIGURE 15-4 Longitudinal (A) and cross-sectional (B) view of the Imatron UFCT scanner.²⁴

In CT units, the heel effect is eliminated by placing the anode–cathode axis of the x-ray tube at right angles to the long axis of the patient.

CT scanners employ compact, high-frequency x-ray generators that are positioned inside the CT gantry. In some units the generator rotates with the x-ray tube, while in others the generator is stationary.

A special x-ray filter is used in CT to make the intensity of the x-ray beam more uniform. This filter is often referred to as “bow-tie filter.”

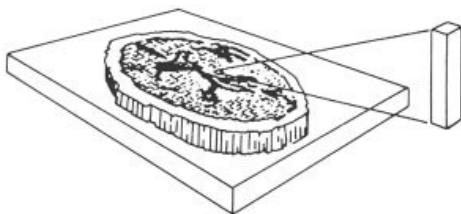
Multislice CT scanning has placed added demands on the capacity of x-ray tubes to sustain high power levels over long periods of time.

The voxel size is the major influence on image resolution in most CT units.

CT units employ two types of collimators: source (prepatient) collimators to shape the x-ray beam and limit patient dose, and detector (postpatient) collimators to control slice thickness.

Reducing CT slice thickness yields the following:

- Decreased partial volume artifact
- Fewer x rays incident upon the detector
- Noisier images



MARGIN FIGURE 15-2
A three-dimensional volume of tissue (voxel) displayed as a two-dimensional element in the CT image (pixel).

High-pressure xenon detectors provide detection efficiencies of about 50%. The detection efficiency of solid-state detectors used in CT is about 80%.

■ X-RAY SOURCES

Both stationary- and rotating-anode x-ray tubes have been used in CT scanners. Many of the translate–rotate CT scanners have an oil-cooled, stationary-anode x-ray tube with a focal spot on the order of 2×16 mm. The limited output of these x-ray tubes necessitates a sampling time of about 5 ms for each measurement of x-ray transmission. This sampling time, together with the time required to move and rotate the source and detector, limits the speed with which data can be accumulated with CT units using translational and rotational motion.

To reduce the sampling time to 2 to 3 ms, newer CT units use 10,000 rpm rotating-anode x-ray tubes, often with a pulsed x-ray beam, to achieve higher x-ray outputs. To meet the demands of high-speed CT scanning, x-ray tubes with ratings in excess of 6 million heat units are becoming standard.

■ COLLIMATION

After transmission through the patient, the x-ray beam is collimated to confine the transmission measurement to a slice with a thickness of a few millimeters. Collimation also serves to reduce scattered radiation to less than 1% of the primary beam intensity. The height of the collimator defines the thickness of the CT slice. This height, when combined with the area of a single picture element (pixel) in the display, defines the three-dimensional volume element (voxel) in the patient corresponding to the two-dimensional pixel of the display.

A voxel encompassing a boundary between two tissue structures (e.g., muscle and bone) yields an attenuation coefficient for the pixel that is intermediate between the values for the two structures. This “partial-volume artifact” may be reduced by narrowing the collimator to yield thinner slices. However, this approach reduces the number of x rays incident upon the detector. With fewer x rays interacting in the detector, the resulting signals are subject to greater statistical fluctuation and yield a noisier image in the final display.

■ X-RAY DETECTORS

To reduce the detector response time, all detectors used in CT are operated in current rather than pulse mode. Also, rejection of scattered radiation is accomplished with detector collimators rather than pulse height analyzers. Detectors for CT scanning, either gas-filled ionization chambers or solid-state detectors, are chosen for their detection efficiency, short response time, and stability of operation. Solid-state detectors include NaI (Tl), CaF₂, and CsI scintillation crystals; ceramic materials containing rare-earth oxides; and bismuth germanate (BGO) and cadmium tungstate [CdWO₄] detectors chosen for their high detection efficiency and low fluorescence decay time. Gas-filled ionization chambers contain xenon pressurized up to 25 atm to improve their x-ray detection efficiency. With any detector, the stability of response from one transmission measurement to the next is essential for production of artifact-free images. With a rotational source and detector geometry, for example, detector instability gives rise to ring-shaped artifacts in the image. Minimum energy dependence of the detectors over the energy range of the x-ray beam is also important if corrections for beam hardening are to be applicable to all patient sizes and configurations.

■ VIEWING SYSTEMS

The numbers computed by the reconstruction algorithm are not exact values of attenuation coefficients. Instead, they are integers termed CT numbers that are related to attenuation coefficients. On most CT units, the CT numbers range from -1000

TABLE 15-2 Electron Densities of Various Body Tissues^a

Tissue	Electron Density (Electrons/cm ³)	Physical Density (g/cm ³)
Water	3.35 × 10 ⁻²³	1.00
Bone	3.72–5.59	1.2–1.8
Spleen	3.52	1.06
Liver	3.51	1.05
Heart	3.46	1.04
Muscle	3.44	1.06
Brain		
White matter	3.42	1.03
Gray matter	3.43	1.04
Kidney	3.42	1.05
Pancreas	3.40	1.02
Fat	3.07	0.92
Lung	0.83	0.25

^aData were calculated from the atomic composition and physical density. Source: Geise and McCullough.²⁵ Used with permission.

for air to +1000 for bone, with the CT number for water set at 0. The relationship between CT number and linear attenuation coefficient μ of a material is

$$CT\ number = 1000 \frac{(\mu - \mu_w)}{\mu_w}$$

where μ_w is the linear attenuation coefficient of water.

CT numbers normalized in this manner provide a range of several CT numbers for a 1% change in attenuation coefficient.

A television monitor is used to portray CT numbers as a gray-scale visual display. This viewing device contains a contrast enhancement feature that superimposes the shades of gray available in the display device (i.e., the dynamic range of the display) over the range of CT numbers of diagnostic interest. Control of image contrast with the contrast enhancement feature is essential in x-ray CT because the electron density, and therefore the x-ray attenuation, are remarkably similar for most tissues of diagnostic interest. This similarity is apparent from the data in Table 15-2. The same cross-sectional CT data displayed at different settings of the “window” of the contrast enhancement control are illustrated in Figure 15-5. The viewing console of the CT scanner may contain auxiliary features such as image magnification, quantitative and statistical data display, and patient identification data. Also, many scanners permit the display of coronal and sagittal images by combining reconstruction data for successive slices through the body.

PATIENT DOSE

The radiation dose delivered during a CT scan is somewhat greater than that administered for an equivalent radiographic image. A CT image of the head requires a dose of about 1 to 2 rad, for example, whereas an abdominal CT image usually requires a dose of 3 to 5 rad. These doses would have to be increased significantly to improve the contrast and spatial resolution of CT images. The relationship between resolution and dose can be approximated as

$$D = a \left(\frac{s^2}{e^3 b} \right) \tag{15-1}$$

where D is the patient dose, s is the signal/noise ratio, e is the spatial resolution, b is the slice thickness, and a is a constant. From Eq. (15-1), the following are apparent:

In a CT image, higher CT numbers are brighter and lower CT numbers are darker.

CT numbers are occasionally, but unofficially, referred to as *Hounsfield units*.

Linear attenuation coefficients of various body tissues for 60 keV x rays.²³

Tissue	M (cm ⁻¹)
Bone	0.528
Blood	0.208
Gray matter	0.212
White matter	0.213
CSF	0.207
Water	0.206
Fat	0.185
Air	0.0004

Filtering of lower-energy x rays from the x-ray beam as it penetrates the patient yields a beam of slightly higher energy in the center of the patient. This effect results in reduced attenuation coefficients in the center compared with the periphery. Hence, the center of the image contains pixels of reduced optical density. This effect is known as the “beam-hardening” artifact.

Image storage devices for CT include magnetic tape and disks, digital videotape, and optical disks and tape.

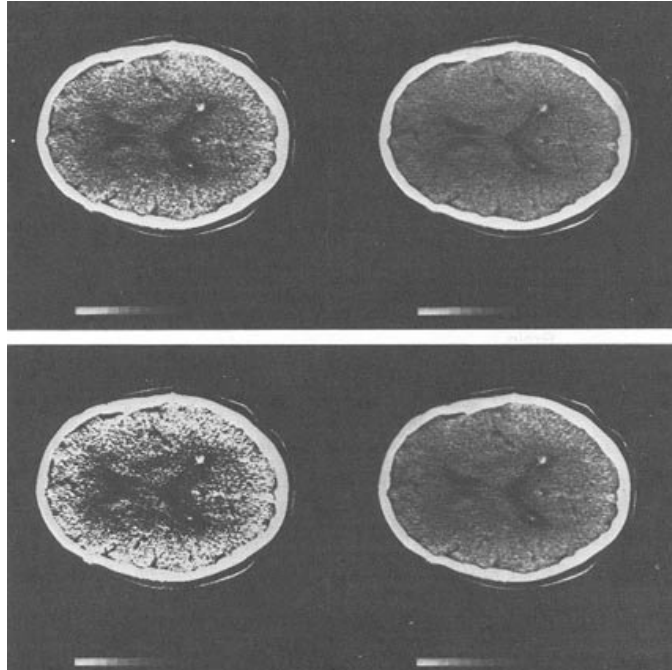


FIGURE 15-5
X-ray attenuation data at four positions of the window level of the contrast enhancement control.

1. A twofold improvement in the signal-to-noise ratio (contrast resolution) requires a fourfold increase in patient dose.
2. A twofold improvement in spatial resolution requires an eightfold increase in patient dose.
3. A twofold reduction in slice thickness requires a twofold increase in patient dose.

In multislice computed tomography, patient dose is described as the CT dose index (CTDI). When the distance that the patient moves between slices (the couch increment CI) equals the slice thickness ST, the CTDI equals the dose averaged over all slices (multislice average dose MSAD). When the couch increment is less than the slice thickness, the MSAD is the CTDI multiplied by the ratio of the slice thickness to the couch increment; that is,

$$\text{MSAD} = \text{CTDI} \left[\frac{\text{ST}}{\text{CI}} \right]$$

Patient dose decreases significantly outside of the slice. A conservative rule of thumb (i.e., an overestimate) is that the dose is 1% of the in-slice dose at an axial distance of 10 cm from the slice.

Techniques for measurement of dose parameters in CT have been described in detail by Cacak.²⁶

In projection radiography, the dose is greatest where the x-ray beam enters the patient. In computed tomography the dose is relatively uniform across the section of tissue exposed to the x-ray beam, because the x-ray beam rotates around the patient during exposure.

■ QUALITY CONTROL

Many electronic components and massive amounts of data processing are involved in producing a CT image. A consequence of the separation between data acquisition and image display is the difficulty of observing and investigating imaging system problems through observation of the image alone. In such a complex system, image quality can be ensured only through prospective monitoring of system components and tests of

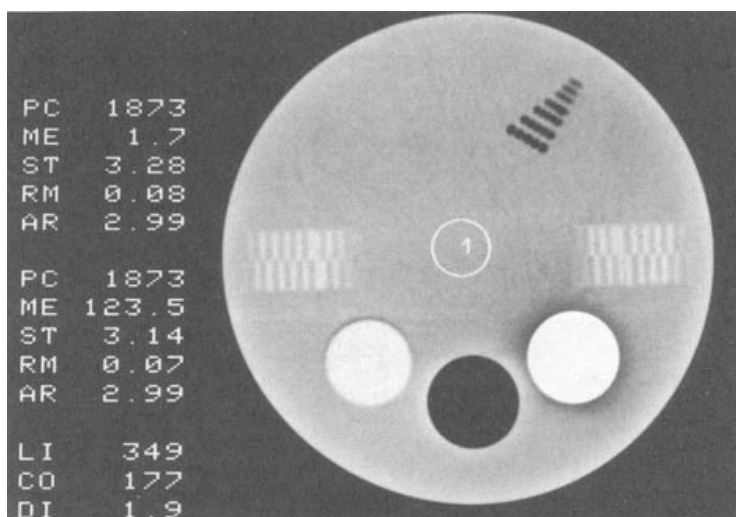


FIGURE 15-6 CT image of a quality control phantom. Image quality is evaluated by analysis of regions of interest and by visual inspection. The mean and standard deviation of pixel values in region 1 indicate CT number calibration, while comparison of region 2 with region 1 yields contrast information. The serrated patterns at 3 and 9 o'clock on the image indicate slice thickness and alignment. The rows of small dark circles (low CT number) at 1 o'clock is an indication of high contrast resolution. (Courtesy of Richard Geise, University of Minnesota Hospital; and Radiation Measurements Incorporated, Middleton, Wisconsin.)

overall system performance with standard phantoms. These measurements should be correlated with patient dose to ensure that the proper balance is maintained among variables that affect contrast, spatial resolution, image noise, and patient radiation dose.

Typical measurements of CT performance are given in Table 15-3, and examples are shown in Figure 15-6. The fundamental system performance indicators are CT number, resolution, noise, and patient dose.²⁶ The accuracy of CT numbers is measured by scanning a water-filled phantom at least monthly. The CT number for water should be zero over a 20-cm-diameter phantom, with a variation of less than 1 CT number. Deviation from the expected CT number of 0 for water at any energy is adjusted by applying a correction factor for the pixel value. Constancy of the value should be monitored with a daily scan.

An overall check of system performance is obtained from semiannual measurements of CT image noise, defined as the standard deviation of CT numbers in a region of interest. Constancy of performance is checked by evaluation of the standard deviation in the daily water scan mentioned previously. Resolution is measured by scanning phantoms on a monthly basis. Of particular importance is low contrast resolution, which is a sensitive indicator of changes in component performance as they affect noise. Patient dose is evaluated semiannually. Specially designed ionization chambers²⁷ provide measurements from which the dose may be calculated for the exposure conditions (narrow beam, variable slice thickness) used in CT.²⁸ The values should agree with manufacturer's specifications to within 20%.

A variety of physical and mechanical factors such as patient couch positioning and indexing should be measured as part of a comprehensive quality control program. The performance of the hard-copy device and system monitors should be checked for distortion, brightness, contrast adjustment, and so on. The accuracy of image analysis features such as distance measurements and measurements of bone density should also be independently evaluated. Additional information on quality control in CT is available in the publications of a number of advisory groups and individuals.²⁹⁻³²

TABLE 15-3 Common Quality Control Measurements for Computed Tomography

Measurement	Frequency
CT number	
Accuracy	Monthly
Constancy check	Daily
Noise	
Evaluation	Semiannually
Constancy check	Daily
Resolution	Monthly
Patient dose	Semiannually

A graph of CT number versus μ should yield a straight line passing through zero for water. This measure, known as the CT number linearity, is essential for quantitative computed tomography.

Reduction in CT number at the center of a water scan is termed "cupping." A heightened CT number at the scan center is known as "peaking." Either result compromises image quality.

SUMMARY

- X-ray transmission CT yields cross-sectional, sagittal, and coronal images with exquisite contrast resolution.
- CT imaging employs the principle of reconstructing images from measurements of x-ray transmission through the body.
- A variety of mathematical models are available for reconstructing x-ray images.
- Special demands are imposed on the x-ray sources and detectors used in CT imaging.
- Quality control and dose limitations are essential features of x-ray CT imaging.

PROBLEMS

- 15-1. Compare the spatial and contrast resolution of conventional radiographic and CT images.
- 15-2. List three reasons why contrast resolution is improved in CT imaging compared with conventional radiographic imaging.
- 15-3. Describe the mechanical features of the four generations of CT scanners.
- 15-4. Briefly describe the simple backprojection approach to image reconstruction, and explain how the convolution method improves these images.
- 15-5. What are the two major constraints on further reductions in CT scan time?
- 15-6. Explain the relationship between a voxel and a pixel.
- 15-7. What types of detectors are used in CT scanners?
- 15-8. Estimate the fetal dose 10 cm from a chest CT examination.
- 15-9. Define a CT (Hounsfield) unit, and explain the purpose of contrast enhancement in a CT viewing device.
- 15-10. Explain how image noise and patient dose in CT scanning are influenced by the signal-to-noise ratio, the size of each resolution element, and the slice thickness.

REFERENCES

1. Bracewell, R. Strip integration in radio astronomy. *Aust. J. Phys.* 1956; **9**:198.
2. DeRosier, D., and Klug, A. Reconstruction of three dimensional structures from electron micrographs. *Nature* 1968; **217**:130.
3. Rowley, P. Quantitative interpretation of three-dimensional weakly refractive phase objectives using holographic interferometry. *J. Opt. Soc. Am.* 1969; **59**:1496.
4. Berry, M., and Gibbs, D. The interpretation of optical projections. *Proc. R. Soc. [A]* 1970; **314**:143.
5. Webb, S. *From the Watching of Shadows*. New York, Adam Hilger, 1990.
6. Oldendorf, W. Isolated flying spot detection of radiodensity discontinuities—displaying the internal structural pattern of a complex object. *IRE Trans. Biomed. Electron.* 1961; **8**:68.
7. Kuhl D, Edwards R. Image separation radioisotope scanning. *Radiology* 1963; **80**:653.
8. Kuhl, D., Hale, J., and Eaton, W. Transmission scanning. A useful adjunct to conventional emission scanning for accurately keying isotope deposition to radiographic anatomy. *Radiology* 1966; **87**:278.
9. Hounsfield, G. Computerized transverse axial scanning (tomography): Part I. Description of system. *Br. J. Radiol.* 1973; **46**:1016.
10. Ledley, R., DiChiro, G., Lussenhop, A., et al. Computerized transaxial x-ray tomography of the human body. *Science* 1974; **186**:207.
11. Hendee, W. *Physical Principles of Computed Tomography*. Boston, Little Brown & Co., 1983.
12. Radon, J. Über die Bestimmung von Funktionen durch ihre Integralwerte laengs gewisser Mannigfaltigkeiten (on the determination of functions from the integrals along certain manifolds). *Ber. Saechs. Akad. Wiss. Leipzig Math. Phys. Kl.* 1917, **69**:262.
13. Korenblyum, B., Tetelbaum, S., and Tyutin, A. About one scheme of tomography. *Bull. Inst. Higher Educ.—Radiophys.* 1958, **1**:151–157.
14. Rowlands, J. X-Ray imaging: Radiography, fluoroscopy, computed tomography, in Hendee, W. (ed.), *Biomedical Uses of Radiation. Part A: Diagnostic Applications*. Weinheim, Germany, Wiley-VCH, 1999.
15. Kalendar, W. A., Seissler, W., Klotz, E., et al. Spiral volumetric CT with single-breathhold technique, continuous transport, and continuous scanner rotation. *Radiology* 1990; **176**:181–183.
16. Hu, H. Multislice helical CT: Scan and reconstruction. *Med. Phys.* 1999; **26**:5.
17. Ritman, E. L., Robb, R. A., Johnson, S. A., et al. Quantitative imaging of the structure and function of the heart, lungs, and circulation. *Mayo Clin. Proc.* 1978; **53**:3–11.
18. Robb, R. A., Hoffman, E. A., Sinak, L. J., et al. High-speed three-dimensional x-ray computed tomography: The dynamic spatial reconstructor. *Proc. IEEE* 1983; **71**:308–319.
19. Robb, R. A., Lent, A. H., and Chu, A. A computer-based system for high-speed three-dimensional imaging of the heart and circulation: Evaluation of performance by simulation and prototype. *Proc. Thirteenth Hawaii Int. Conf. System Sci.* 1980; **III**:384–405.
20. Boyd, D. P., Lipton, M. J. Cardiac computed tomography. *Proc. IEEE* 1983; **71**:308–319.
21. Linuma, T. A., Tateno, Y., Umegake, Y., et al. Proposed system for ultra-fast computed tomography. *J. Comput. Assist. Tomogr.* 1977; **1**:494–499.
22. Peschmann, K. R., Napel, S., Couch, J. L., et al. High-speed computed tomography: Systems and performance. *Appl. Opt.* 1985; **24**:4052–4060.
23. Seeram, E. *Computed Tomography*. Philadelphia, W. B. Saunders, 2001, p. 66.
24. Gould, R. G. Computed tomography overview and basics, in *Specification, Acceptance Testing and Quality Control of Diagnostic X-Ray Imaging Equipment*, Proceedings of the American Association of Physicists in Medicine, Vol. 2. Santa Cruz, Calif, July 1991, pp. 930–968.

25. Geise, R. A., and McCullough, E. C. The use of CT scanners in megavoltage photon-beam therapy planning. *Radiology* 1977; **124**:133–141.
26. Cacak, R. K. Measuring patient dose from computed tomography scanners, in Seeram, E. (ed.), *Computed Tomography*. Philadelphia, W. B. Saunders, 2001, pp. 199–208.
27. Moore, M. M., Cacak, R. K., and Hendee, W. R. Multisegmented ion chamber for CT scanner dosimetry. *Med. Phys.* 1981; **8**:640–645.
28. Shope, T. B., Gagne, R. M., Johnson, G. D. A method of describing the doses delivered by transmission x-ray computed tomography. *Med. Phys.* 1981; **8**:488–495.
29. National Council on Radiation Protection and Measurements. *Quality Assurance for Diagnostic Imaging Equipment*. Report 99. Bethesda, MD, NCRP, 1988.
30. American College of Medical Physics. *Radiation Control and Quality Assurance Surveys*, Report no. 1. Reston, VA, American College of Medical Physics, 1986.
31. Cacak, R. K. Design of a quality assurance program: CT scanners, in Hendee, W. R. (ed.), *Selection and Performance Evaluation of Radiologic Equipment*. Baltimore, Williams & Wilkins, 1985.
32. Cacak, R. K. Quality control for computed tomography scanners, in Seeram, E. (ed.), *Computed Tomography*. Philadelphia, W. B. Saunders, 2001, pp. 385–407.